

Supplemental Materials

Contents

Experimental details	2
<i>Fig. 5C.</i>	2
Supplemental Figure legends, Busso et al.	2
<i>Fig. S1. Expression and purification of recombinant muAPE1</i>	2
<i>Fig. S2. Expression vectors with a single FRT integration site</i>	3
<i>Fig. S3. Effect of ubiquitination on APE1's repair function</i>	3
<i>(A-E) Effect of ubiquitination on APE1's affinity for DNA</i>	3
<i>Fig. S4. Construction of KallR APE1 cDNA</i>	4
<i>Fig. S5. Role of MDM2 and CDK5 for APE1 ubiquitination in cells.</i>	5
<i>Fig. S6. Evaluation of gene expression array results</i>	5

Experimental details

Fig. 5C.

For formaldehyde (FA) cross-linking assay, the procedure in Current Protocols in Molecular Biology (basic protocol 2 in Chapter 21.3) was used. Cells were treated with FA (final 1%) for 8 min at room temperature and then quenched with 0.4 M glycine. Cells were then centrifuged, washed in ice-cold TBS buffer (100 mM Tris 7.5, 150 mM NaCl), resuspended in MC buffer (10 mM Tris pH 7.5, 10 mM NaCl, 3 mM MgCl₂, 0.5% NP-40), and then equal volume of x2 MNase buffer (10 mM Tris pH7.5, 10 mM NaCl, 3 mM MgCl₂, 1 mM CaCl₂, 4% NP-40) was added to the cell suspension. The cells were sonicated for 10 seconds to lyse the cellular membranes. This short sonication procedure was to ensure the genomic DNA was not sheered to short fragments. Soluble proteins were separated from the total fraction by centrifugation (30 min at maximum speed in a microcentrifuge) at 4°C. The total and soluble fractions were analyzed for the presence of uAPE1 and iAPE1.

Supplemental Figure legends, Busso et al.

Fig. S1. Expression and purification of recombinant muAPE1

(A) Expression and purification of recombinant muAPE1. (Left panel) *E. coli* BLR(DE3) (Novagen) was transformed with 3 expression vectors to express human uba1 in pACYC-Duet1, ubch5b and MDM2 in pRSF-Duet1, ubiquitin with (right) or without (left) APE1 in pET-Duet1. S: total soluble fractions of IPTG-induced cells, F: flow-through of column chromatography of Ni-NTA resin, W: 20 mM imidazole wash, E: eluted with 200 mM. Filled arrow: muAPE1. Samples were analyzed in IB using an APE1 antibody. Unmodified, intact APE1 in fraction E (open arrow, right most lane) was most likely due to intrinsic affinity of APE1 for the nickel resin. **(Right panel)** Recombinant muAPE1 fraction prepared as in the right panel (lane 1) was compared to uAPE1 generated by T233E APE1 transfection in HCT116 sh-

Ctl (Fig. 1). The size of recombinant muAPE1 matches with one of uAPE1 band (single arrow), with a slight upper shift due to the His-tag portion in the recombinant muAPE1 (about 1kDa difference). Arrow: position of muAPE1, double arrow: position of di-ubiquitinated APE1, filled circle: recombinant muAPE1, and open circle: intact (unmodified) recombinant APE1. **(B)** Interaction between APE1 and MDM2. BLR(DE3) expressing MDM2 (1-6) and wtAPE1 (1&4), wtAPE1-FLAG (2&5), T233E APE1-FLAG (3&6). 1-3: total fraction; 4-6: FLAG-immunoprecipitates. Top, MDM2; Bot, APE1.

Fig. S2. Expression vectors with a single FRT integration site

(A) pcDNA5.1/FRT/TO vector (Invitrogen). **(B)** the wtAPE1 cDNA inserted into *HindIII-XhoI*. **(C)** the G76A Ub fused to Lys24 of APE1. A strong nuclear localization signal (NLS) from SV40 large T antigen was placed at the N-terminus. **(D)** nuclear localization of the NLSUbAPE1 **(c)** stained with FITC **(F)** in mouse NIH3T3 cells. DAPI **(D)** and MitoTracker **(M)** were co-stained and merged **(X)**.

Fig. S3. Effect of ubiquitination on APE1's repair function

(A-E) Effect of ubiquitination on APE1's affinity for DNA

(A) SDS/PAGE-Coomassie staining showing purified intact APE1 and Ub-APE1 fusion proteins. The pET15b derivatives expression corresponding APE1 proteins were induced with 0.5 mM IPTG and purified with Ni-NTA columns as previously (1). **(B)** Fluorescence anisotropy assays carried out with variable concentrations (0 - 2000 nM) of APE1 as indicated in x-axis and 10 nM 21-mer duplex DNA labeled with fluorescein at its 5'-end. The sequence of oligonucleotide (top) was: CGCTTGATGAGTCAGCCGGAA. The proteins and DNA were incubated in 50 mM HEPES 7.5, 1 mM EDTA, 6 mM CaCl₂ with variable NaCl concentration as

indicated for 3 min and fluorescence anisotropy was measured in Varian Eclipse with excitation/emission = 480 nm/520 nm (slit size = 10 nm) at 900V. **(C)** K_d of both proteins at corresponding salt concentrations were calculated by non-linear regression analysis (Mathematica) using the equation (2) for 1:1 DNA:APE1 binding. **(D)** SDS/PAGE-Coomassie staining showing purified ubiquitin protein purchased from Sigma. **(E)** Fluorescence anisotropy of 10 nM duplex oligonucleotide with variable concentration of ubiquitin, resulting in no response, indicating that ubiquitin has any detectable affinity for DNA.

(F) Effect of ubiquitination on APE1's repair reaction in *E. coli* cells.

To examine the effect of APE1 ubiquitination on AP-endonuclease activity, *E. coli* BW535, a double APE-negative mutant (*xthA nfo nth*) that were harboring an empty vector (vec, triangle), the wtAPE1 gene (wtAPE1, circle), or the Ub-APE1 fusion gene (Ub-APE1, square), was grown in LB broth at 28°C to logarithmic growth phase (until optical density reached about 0.3) with 12.5 μg/ml kanamycin and 50 μg/ml ampicillin. Resuspended in PBS, cells were treated with indicated concentration of methyl methanesulfonate (MMS, an alkylating reagent that facilitates DNA depurination) at 37°C for 1 h with vigorous shaking to generate AP sites in cells. Cells were then plated on LB agar plates after appropriate dilutions in PBS, and surviving colonies were counted. Average and standard deviation were calculated based on three or more independent platings. The plasmid vector, pIZ42, is a derivative of pBluescript SK(-) (Stratagene) used in a previous study (3).

Fig. S4. Construction of KallR APE1 cDNA

(A) KallR APE1 is a full-length APE1 with T233E missense, and all 27 Lys residues in the wt-APE1 is converted to Arg. The clone was created by a PCR buildup method, using 50 short nucleotides shown in this figure. All oligonucleotides (50 pmol) were mixed in a 50 μl PCR reaction mixture, and then PCR was carried out using Phusion Taq polymerase (NEB).

Resulting DNA was cloned into pCDNA3.1Zeo, and its sequence was confirmed by direct sequencing. **(B)** KallR APE1 analyzed in immunoblot. HCT116 transfected with vector (lane 1), KallR (lane 2), KallR with N-terminal x6 His fusion (lane 3), and KallR with C-terminal x6 His fusion (lane 4). The Lys-less APE1 migrates faster than the wild-type APE1 (lane 2, arrow). Slower migrations of the N-terminally or C-terminally tagged proteins (3&4, arrows) than KallR (2) indicate that both ends of KallR protein are intact.

Fig. S5. Role of MDM2 and CDK5 for APE1 ubiquitination in cells.

(A) MDM2^{-/-} MEF cells were transfected with the vector (1) or the wtAPE1, MDM2, and ubiquitin genes (2-5). After 24 h, cells were treated with MG132 for 3 h (4) or 5 h (5), and then analyzed for ubiquitinated as well as intact APE1. **(B)** HCT116 cells were transfected with the wtAPE1, MDM2, and G76A ubiquitin. After 24 h, cells were treated with 10 μ M roscovitine (Sigma) for 3 h, and then cell lysates were processed for His-tag purification and analyzed with anti-APE1 antibody.

Fig. S6. Evaluation of gene expression array results

(A) The genes resulting p-value of less than 0.05 based on Welch ANOVA (about 15,000 total) were pooled and fold increase/decrease was calculated for each gene and plotted in the histograms. The values are given in logarithmic, i.e., the intensity change is given as:

$$Fold\ change = \text{Log} \left\{ \frac{(Intensity\ of\ a\ gene\ with\ dox)}{(Intensity\ of\ a\ gene\ without\ dox)} \right\}$$

Based on the histogram plots, skewness and kurtosis values were calculated for each cell line by calculating the third and fourth moment of the mean values. **(B)** RT-PCR was carried out for three genes: ferritin, YBX1 (Y box binding protein 1), and TUB1a (tubulin alpha 1a). Results of Affymetrix gene expression array indicated that these three genes were suppressed when ub-APE1 fusion protein was expressed. The 293 T-Rex Flp cells with the wt-APE1 or

ub-APE1 under the doxycycline (dox) control were plated one day before the treatment with 2 $\mu\text{g/ml}$ dox for 16 h. Total RNA was extracted from the cells with or without dox, and subjected to RT-PCR using ABI TaqMan RTPCR probes in triplicates using in Bio-Rad CFX96/C-1000 Thermocycler. Probes used are Hs01000478_g1, Hs00898625_g1, Hs00897656_g1 for ferritin, YBX1, TUB1a, respectively. Results were normalized with beta-actin probe (4333762F), and induction (or suppression) by dox were calculated in the plot.

(C) Genes previously described (4) and were found in this study to be activated by the induction of wtAPE1, but suppressed by the induction of ub-APE1. The genes are categorized based on the previous study (4). Five categories are:

Category 1: Cell cycle, growth and maintenance and apoptosis;

Category 2: Cell adhesion, signal transduction, cell-cell signaling and chaperones;

Category 3: Transcription factors, chromatin factors and DNA-repair enzymes;

Category 4: Protein synthesis and metabolism related;

Category 5: Ion channels and redox associated proteins.

References

1. Mol,C.D., Izumi,T., Mitra,S. and Tainer,J.A. (2000) DNA-bound structures and mutants reveal abasic DNA binding by APE1 and DNA repair coordination [corrected] *Nature* **403**, 451-456.
2. Heyduk,T. and Lee,J.C. (1990) Application of fluorescence energy transfer and polarization to monitor Escherichia coli cAMP receptor protein and lac promoter interaction. *Proc Natl Acad Sci U S A* **87**, 1744-1748.
3. Izumi,T. and Mitra,S. (1998) Deletion analysis of human AP-endonuclease: minimum sequence required for the endonuclease activity. *Carcinogenesis* **19**, 525-527.
4. Vascotto,C., Fantini,D., Romanello,M., Cesaratto,L., Deganuto,M., Leonardi,A., Radicella,J.P., Kelley,M.R., D'Ambrosio,C., Scaloni,A., Quadrifoglio,F. and Tell,G. (2009) APE1/Ref-1 interacts with NPM1 within nucleoli and plays a role in the rRNA quality control process. *Mol Cell Biol* **29**, 1834-1854.

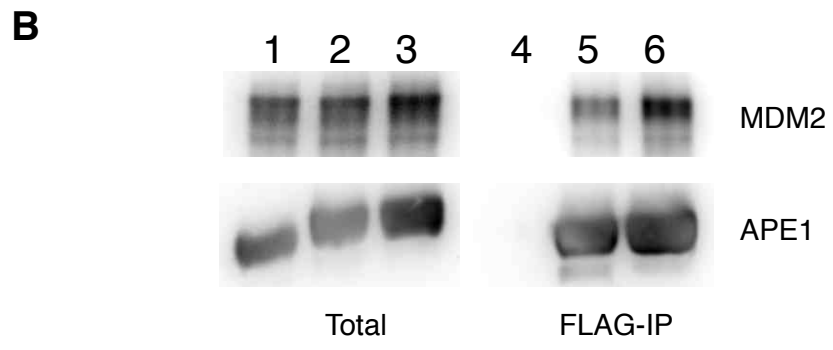
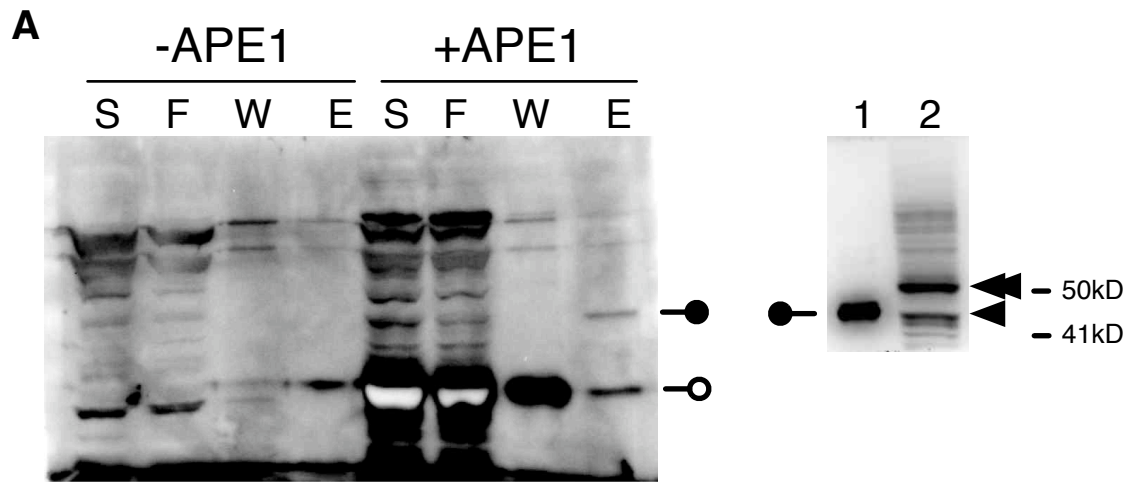


Fig. S1. Busso, et al.

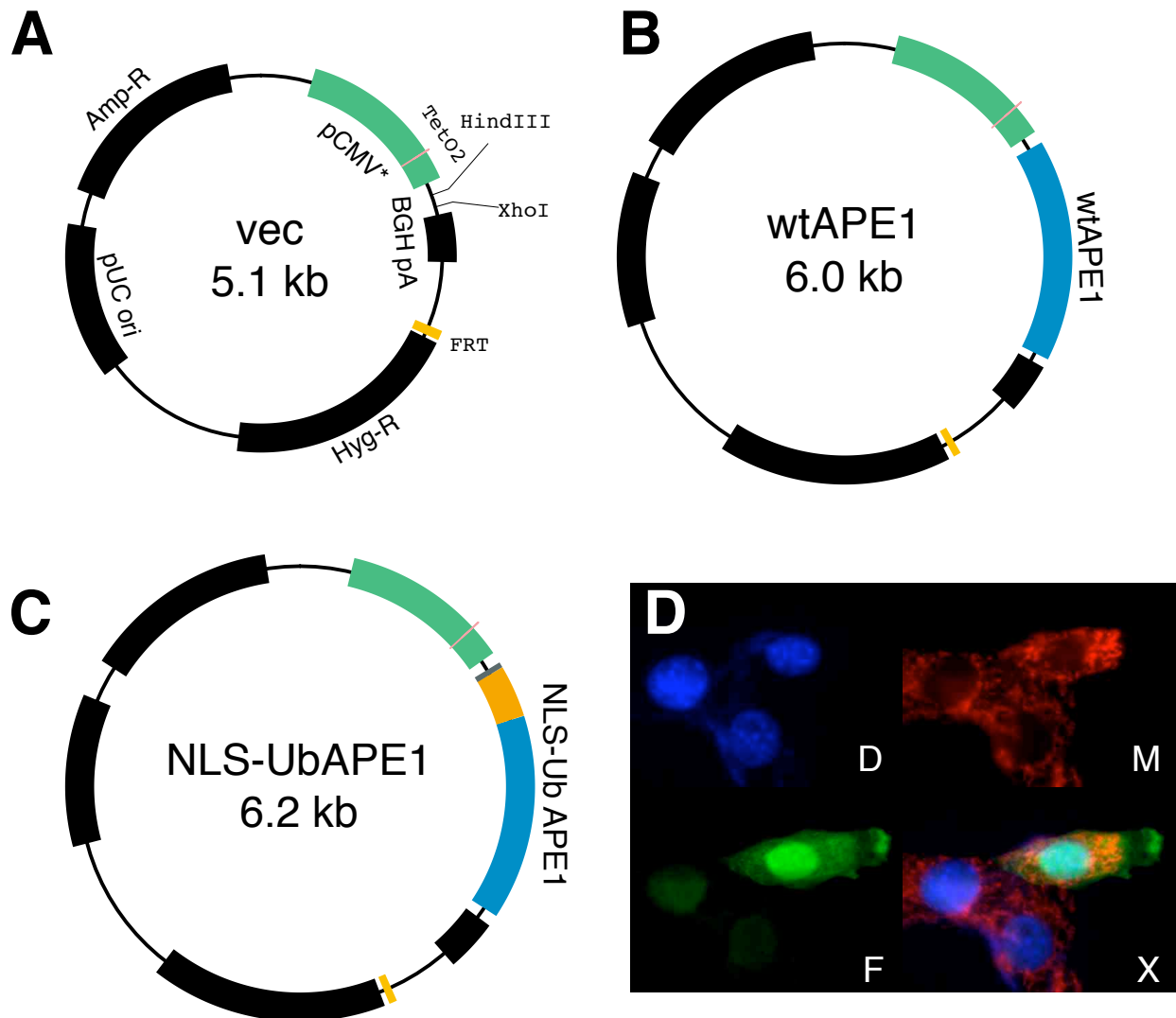
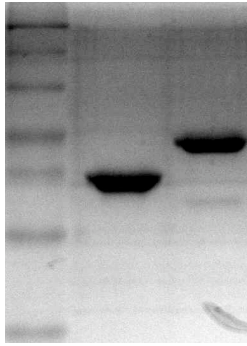
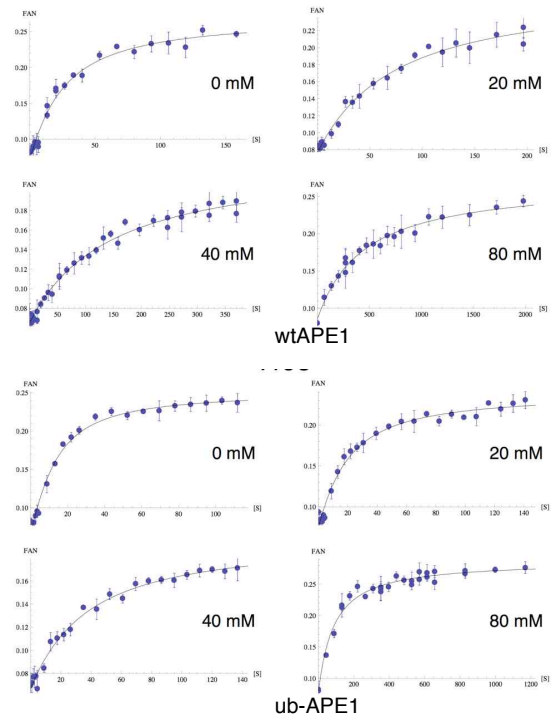


Fig. S2. Busso, et al.

A**B****C**

NaCl (mM)	Kd (nM)	
	wtAPE1	ub-APE1
0	20.4±2.3	8.21±0.8
20	67.7±7.71	14.7±1.58
40	137.5±11.5	31.4±3.1
80	442.4±40.2	81.5±6.4

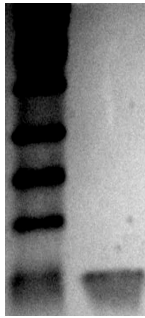
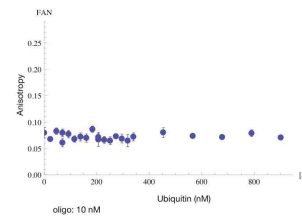
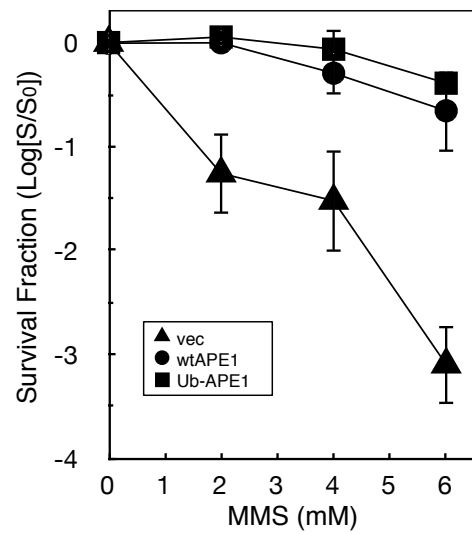
D**E****F**

Fig. S3. Busso, et al.

A

Name	Sequence (5'-3')
Top_1	TTA TGG ATC CAC CAT GCC GCG GCG TGG GAG GAG GGG AGC G
Top_2	GTG GCG GAA GAC GGG GAT GAG CTC AGG ACA GAG CCA GAG G
Top_3	CCC GGC GCA GTA GGA CGG CCG CAA GGC GCA ATG ACA GGG A
Top_4	GGC AGC AGG AGA GGG CCC AGC CCT GTA TGA GGA CCC CCC A
Top_5	GAT CAG CGC ACC TCA CCC AGT GGC AGG CCT GCC ACA CTC C
Top_6	GGA TCT GCT CTT GGA ATG TGG ATG GGC TTC GAG CCT GGA T
Top_7	TAG ACG CCG CGG ATT AGA TTG GGT AAG GGA AGA AGC CCC A
Top_8	GAT ATA CTG TGC CTT CAA GAG ACC CGA TGT TCA GAG AAC A
Top_9	GGC TAC CAG CTG AAC TTC AGG AGC TGC CTG GAC TCT CTC A
Top_10	TCA ATA CTG GTC AGC TCC TTC GGA CCG GGA AGG GTA CAG T
Top_11	GGC GTG GGC CTG CTT TCC CGC CAG TGC CCA CTC CGC GTT T
Top_12	CTT ACG GCA TAG GCG ATG AGG AGC ATG ATC AGG AAG GCC G
Top_13	GGT GAT TGT GGC TGA ATT TGA CTC GTT TGT GCT GGT AAC A
Top_14	GCA TAT GTA CCT AAT GCA GGC CGA GGT CTG GTA CGT G
Top_15	AGT ACC GGC AGC GCT GGG ATG AAG CCT TTC GCA GGT TCC T
Top_16	GAG AGG CCT GGC TFC CCG ACG GCC CCT TGT GCT GTG TGG A
Top_17	GAC CTC AAT GTG GCA CAT GAA GAA ATT GAC CTT CGC AAC C
Top_18	CCA GGG GGA ACC GAC GGA ATG CCG GCT TCG AGC CAC AAG A
Top_19	GCG CCA AGG CTT CGG GGA ATT ACT GCA GGC TGT GCC ACT G
Top_20	GCT GAC AGC TTT AGG CAC CTC TAC CCC AAC ACA CCC TAT G
Top_21	CCT ACA CCT TTT GGA CTT ATA TGA TGA ATG CTC GAT CCA G
Top_22	AAA TGT TGG TTG GCG CCT TGA TTA CTT TTT GTT GTC CCA C
Top_23	TCT CTG TTA CCT GCA TTG TGT GAC AGC CGG ATC CGT TCC A
Top_24	GGG CCC TCG GCA GTG ATC ACT GTC CTA TCA CCC TAT ACC T
Top_25	AGC ACT GTG ACT CGA GTT AT
Bot_1	GCG GCA TGG TGG ATC CAT AA
Bot_2	TCA TCC CCG TCT TCC GCC ACC GCT CCC CTC CTC CCA CGC C
Bot_3	GGC CGT CCT ACT GCG CCG GGC CTC TGG CTC TGT CCT GAG C
Bot_4	CTG GGC CCT CTC CTG CTG CCT CCC TGT CAT TGC GCC TTG C
Bot_5	CTG GGT GAG GTG CGC TGA TCT GGG GGG TCC TCA TAC AGG G
Bot_6	CAC ATT CCA AGA GCA GAT CCG GAG TGT GGC AGG CCT GCC A
Bot_7	AAT CTA ATC CGC GGC GTC TAA TCC AGG CTC GAA GCC CAT C
Bot_8	TCT TGA AGG CAC AGT ATA TCT GGG GCT TCT TCC CTT ACC C
Bot_9	CTG AAG TTC AGC TGG TAG CCT GTT CTC TGA ACA TCG GGT C
Bot_10	AAG GAG CTG ACC AGT ATT GAT GAG AGA GTC CAG GCA GCT C
Bot_11	CGG GAA AGC AGG CCC ACG CCA CTG TAC CCT TCC CGG TCC G
Bot_12	CTC ATC GCC TAT GCC GTA AGA AAC GCG GAG TGG GCA CTG G
Bot_13	CAA ATT CAG CCA CAA TCA CCC GGC CTT CCT GAT CAT GCT C
Bot_14	CCT GCA TTA GGT ACA TAT GCT GTT ACC AGC ACA AAC GAG T
Bot_15	ATC CCA GCG CTG CCG GTA CTC CAG TCG TAC CAG ACC TCG G
Bot_16	GTC GGG AAG CCA GGC CTC TCA GGA ACC TGC GAA AGG CTT C
Bot_17	TCA TGT GCC ACA TTG AGG TCT CCA CAC AGC ACA AGG GGC C
Bot_18	ATT CCG TCG GTT CCC CCT GGG GTT GCG AAG GTC AAT TTC T
Bot_19	ATT CCC CGA AGC CTT GGC GCT CTT GTG GCT CGA AGC CGC C
Bot_20	AGG TGC CTA AAG CTG TCA GCC AGT GGC ACA GCC TGC AGT A
Bot_21	ATA AGT CCA AAA GGT GTA GGC ATA GGG TGT GTT GGG GTA G
Bot_22	CAA GGC GCC AAC CAA CAT TTC TGG ATC GAG CAT TCA TCA T
Bot_23	CAC AAT GCA GGT AAC AGA GAG TGG GAC AAC AAA AAG TAA T
Bot_24	GTG ATC ACT GCC GAG GGC CCT GGA ACG GAT CCG GCT GTC A
Bot_25	ATA ACT CGA GTC ACA GTG CTA GGT ATA GGG TGA TAG GAC A

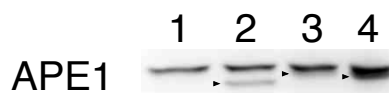
B

Fig. S4. Busso, et al.

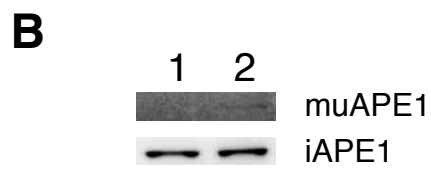
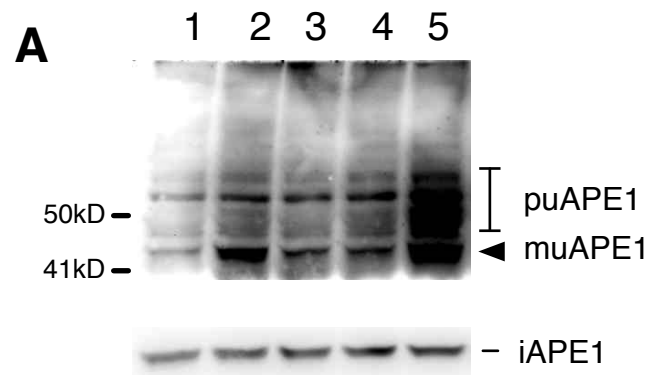


Fig. S5. Busso, et al.

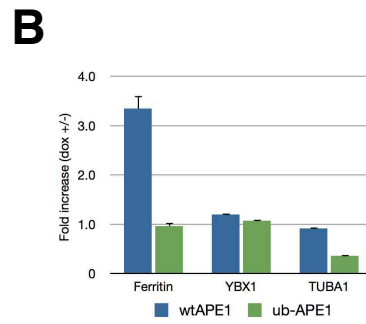
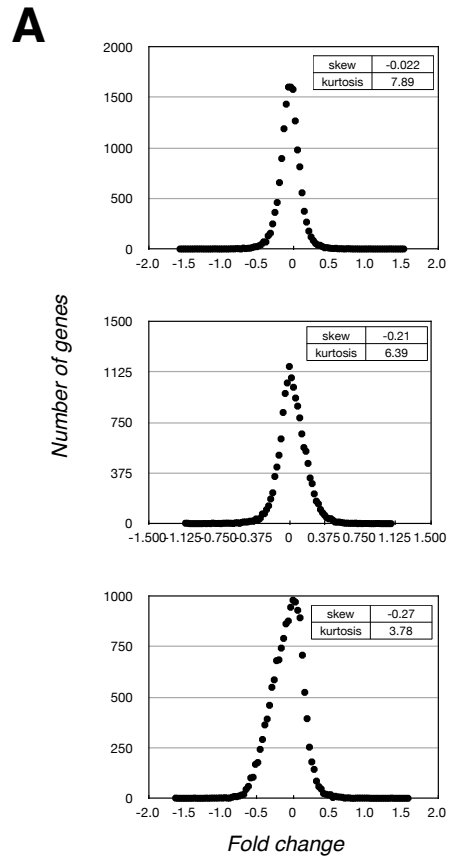


Fig. S6. Busso, et al.

C

Category	fold increase by induction of either w/APE1 or ub-APE1		Gene	Gene ID
	w/APE1	ub-APE1		
1	1.21	0.78	apoptosis inhibitor 5, API5	NM_006595 // GO:0005634 //
	1.24	0.78	cell division cycle associated 7, CDCA7	NM_031942 // GO:0005634 //
	1.36	1.05	CDC45 cell division cycle 45-like (S. cerevisiae), CDC45L	NM_003504 // GO:0005634 //
	1.29	0.67	cyclin E2, CCNE2	NM_057749 // GO:0005634 //
	1.30	1.05	adaptor-related protein complex 1, sigma 2 subunit	AF087876 BX537780
2	1.39	1.00	PRKAG1	NM_212461 // GO:0005634 //
	1.20	0.95	SUMO1 activating enzyme subunit 1, SAE1	NM_005500 // GO:0005634 //
	1.11	0.61	IL6ST	NM_002184 // GO:000576 //
	1.65	1.37	heat-responsive protein 12, HRSP12	NM_005836 // GO:0005634 //
	1.13	0.65	calcium binding protein 39, CAB39	NM_016289 // GO:0005737 //
3	1.45	0.87	NFAT5	NM_138714 // GO:0005634 //
	1.14	0.71	polymerase (DNA-directed), alpha 1 small Cajal body-specific RNA 23	AF085825 BX648513
	1.62	1.15	polymerase (DNA-directed), delta 3, main	NM_006591 // GO:0005634 //
	1.52	0.96	methylentetrahydrofolate dehydrogenase (NADP+ dependent) 1, methylentetrahydrofolate cyclohydrolase, main	NM_005956 // GO:0005737 //
	1.77	1.21	eukaryotic translation initiation factor 2, subunit 3 gamma, main	NM_001415 // GO:0005850 //
4	1.34	1.05	glutamic-oxaloacetic transaminase 1, soluble (aspartate aminotransferase 1)	DQ372724
	1.85	1.24	HERPUD1	NM_014685 // GO:0005783 //
	1.61	1.35	transaldolase 1, TALDO1	NM_006755 // GO:0005737 //
5	1.66	0.88	PRDX3	NM_006793 // GO:0005739 //